Krishna *et al. Applied Biological Chemistry* (2023) 66:37
https://doi.org/10.1186/s13765-023-00795-1

KSABC
The Korean Society for Applied Biological Chemistry

ARTICLE Open Access

Inhibition of monoamine oxidases by benzimidazole chalcone derivatives

Athulya Krishna[1†], Jiseong Lee[2†], Sunil Kumar[1], Sachithra Thazhathuveedu Sudevan[1], Prerna Uniyal[3], Leena K. Pappachen[1*], Hoon Kim[2*] and Bijo Mathew[1*]

Abstract

Ten benzimidazole chalcone derivatives were synthesized, and their monoamine oxidase (MAO) inhibitory activity was evaluated. Most compounds showed higher inhibitory activity against MAO-B than MAO-A. Compound BCH2 exhibited an IC_{50} value of 0.80 μM, thereby showing the most potent inhibition amongst all. In addition, BCH2 showed the highest MAO-B selectivity index (SI) with an SI value of 44.11 compared to MAO-A. Among the substituents, the halogen group showed the best MAO-B inhibition, and the *ortho*-position of the B ring showed better inhibitory activity than the *para*-site. In comparison with *ortho*-substituents, the inhibitory activity increased in the order, -Cl > -Br > -F > -H. BCH2 was found to be a competitive inhibitor of the enzyme with optimum inhibition kinetics, where K_i was found to be 0.25 ± 0.014 μM. In the reversibility experiment, BCH2 showed a recovery pattern after MAO-B inhibition, similar to that of lazabemide. Thus, BCH2 is a potent, reversible, and selective MAO-B inhibitor and has been suggested as a candidate for the treatment of neurological disorders.

Keywords Benzimidazole, Chalcones, MAO-A, MAO-B, Kinetics, Molecular docking

Introduction

Alzheimer's disease (AD) is a prominent neurodegenerative condition that causes dementia and impairs intellectual performance. Amyloid plaques and intracellular neurofibrillary tangles (NFTs) built in the brain of AD patients, which inevitably lead to cerebral atrophy. Elevated oxidative stress is detected in the initial phases of AD, implying a surge in reactive oxygen species (ROS) [1]. Monoamine oxidases (MAOs) play a significant role in ROS production by facilitating oxidative deamination, resulting in the production of H_2O_2, an ROS that is a key contributor to the development of oxidative stress [2–4]. The two MAO isoforms, MAO-A and MAO-B, are generated by distinct genes and exhibit different substrate preferences. The brains of patients with AD have higher levels of MAO-B expression than the typical human brain, which results in the production of ROS and enhances the metabolism of monoamine neurotransmitters such as dopamine, both of which exacerbate the symptoms of the disease [5].

Due to its pathological and pharmacological properties, MAO-B is a promising target for AD therapy. Selegiline, rasagiline, and safinamide are the three main MAO-B inhibitors currently available in the market. While the former two are irreversible MAO-B inhibitors, the latter is a reversible MAO-B inhibitor. All these medications are used in the management of neurological disorders

†Athulya Krishna and Jiseong Lee contributed equally to this work.

*Correspondence:
Leena K. Pappachen
leenakpappachen@pharmacy.aims.amrita.edu
Hoon Kim
hoon@sunchon.ac.kr
Bijo Mathew
bijomathew@aims.amrita.edu; bijovilaventgu@gmail.com
[1] Department of Pharmaceutical Chemistry, Amrita School of Pharmacy, AIMS Health Sciences Campus, Amrita Vishwa Vidyapeetham, Kochi 682 041, India
[2] Department of Pharmacy, and Research Institute of Life Pharmaceutical Sciences, Sunchon National University, Suncheon 57922, Republic of Korea
[3] School of Pharmacy, Graphic Era Hill University, Dehradun 248002, Uttarakhand, India

because of their ability to prevent dopamine degradation [6–8].

Benzimidazole is regarded as a useful compound because of its presence in a diverse range of bioactive molecules. Benzimidazole is a bicyclic heteroaromatic compound with imidazole and benzene rings fused at positions 4 and 5. The first benzimidazole synthesis was reported by Hoebrecker through the reduction of 2-nitro-4-methyl acetanilide in 1872 [9]. Benzimidazole exhibits both acidic and basic properties; its NH group is highly acidic and mildly basic. Various benzimidazole derivatives display different pharmacological activities, including anti-inflammatory, antifungal, antituberculosis, anticancer, antimalarial, antihistamine, antiviral, and antidiabetic. Due to these variations in pharmacological actions, several FDA-approved drugs have been developed based on benzimidazole scaffold, which includes azilsartan (angiotensin II receptor blocker), albendazole (anthelmintic agent), esomeprazole (proton pump inhibitors), benperidol (antipsychotic), bezitramide (opioid), astemizole (antihistamine), benomyl (fungicide), and nocodazole (anticancer agent) (Fig. 1) [10–12].

Since chalcones are a biosynthetic precursor of flavonoids, they are known as open-chain flavonoids and are chemically α,β-unsaturated ketones consisting of two aromatic rings joined by an unsaturated three-carbon system. The presence of three rotatable bonds in the structure enables chalcones to have more flexibility, which contributes to a variety of pharmacological activities, including neuroprotective and MAO-B inhibitory

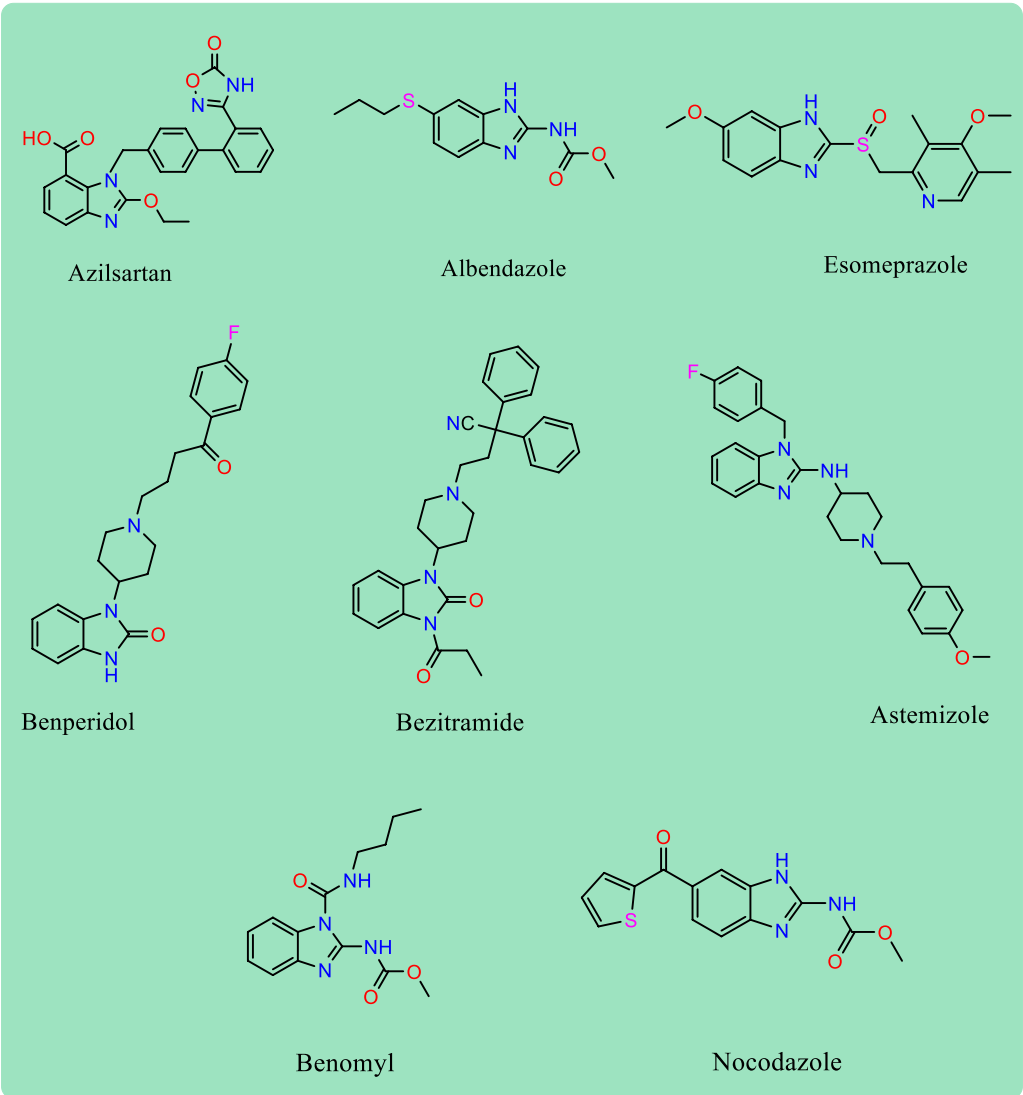

Fig. 1 Structure of FDA-approved drugs containing benzimidazole scaffold

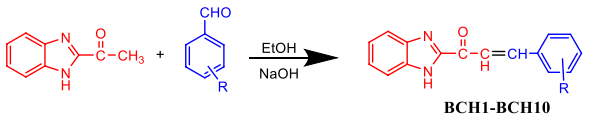

Code	R	Code	R
BCH1	H	BCH6	2-F
BCH2	2-Cl	BCH7	4-F
BCH3	4-Cl	BCH8	4-C_2H_5
BCH4	2-Br	BCH9	4-CH_3
BCH5	4-Br	BCH510	4-OCH_3

Scheme 1 Synthesis of benzimidazole chalcones

activity [13–18]. Thus, several studies have been conducted on the modification of the chalcone scaffold to examine the outcome of substitutions on the effectiveness of the molecule. In particular, halogen substitutions have been extensively studied owing to their lipophilic nature [19, 20]. In the current study, 10 benzimidazole-based chalcone compounds (BCH) were synthesized, and their MAO inhibitory activities were assessed. Ring A of the chalcone was replaced with a heterocyclic benzimidazole ring, and ring B was substituted with various electron-withdrawing and electron-donating groups.

Materials and methods

Synthesis

Equimolar quantities of 2-acetyl benzimidazole and *ortho-* or *para*-substituted benzaldehyde were dissolved in 20 mL of ethanol and 40% KOH (7.5 mL). The reaction mixture was then allowed to stir for 24 h on a magnetic stirrer. The obtained mixture was poured into crushed ice, and the precipitate was filtered. After drying, the products were recrystallized from methanol. All reactions were monitored by performing thin-layer chromatography using hexane and ethyl acetate (2:0.5, v/v) as the mobile phase (Scheme 1). All molecules were previously synthesized and reported by our research group [21–23].

MAO inhibition study

Chemicals for MAO inhibition

Recombinant human MAO-A, MAO-B, benzylamine, kynuramine, pargyline, lazabemide, clorgyline, and toloxatone were purchased from Sigma-Aldrich (St. Louis, MO, USA). Mono- and dibasic anhydrous sodium phosphates were purchased from Daejung Chemicals & Metals Co Ltd (Siheung, Korea). Dialyzer (6–8 kDa, DiaEasy™) was purchased from BioVision (St. Grove, MA, USA) [24].

Inhibition studies of MAO-A and MAO-B

MAO-A and MAO-B were assayed for activities; the experiments were conducted by adding 0.06 mM of kynuramine and 0.3 mM of benzylamine as substrates, respectively. To determine the activity of each enzyme, changes in absorbance were continuously measured at 316 and 250 nm. Toloxatone, clorgyline, lazabemide, and pargyline were used as reference compounds for comparison with the inhibitor compounds [25].

Enzyme kinetics

Residual activity was evaluated at 10 µM during an initial activity screening, and IC_{50} values were determined for potential compounds having IC_{50} below 40 µM with the help of GraphPad Prism software 5 (San Diego, CA, USA) [26]. The selectivity index (SI) value of MAO-B was calculated using the formula, IC_{50} of MAO-A / IC_{50} of MAO-B [27]. The types of enzyme inhibition of MAO-A and MAO-B were determined at five different substrate concentrations (0.0075–0.12 and 0.0375–0.6 µM, respectively) and three inhibitor concentrations (~ 1/2 x, 1 x, and 2×IC_{50}) [28]. The enzyme kinetic patterns and K_i values were determined by comparing Lineweaver–Burk plots and their secondary plots, respectively [29].

Reversibility studies

The reversibility of MAO-A and MAO-B inhibition was evaluated by comparing undialyzed and dialyzed residual activities at a concentration two times the IC_{50} after pre-incubation for 30 min, as described previously [30]. Two types of reference inhibitors were used for MAO-A and MAO-B: the reversible inhibitors toloxatone and lazabemide (MAO-A and MAO-B, respectively), and the irreversible inhibitors clorgyline and pargyline (MAO-A and MAO-B inhibitors, respectively). The reversibility patterns were determined by comparing the activities of undialyzed (A_U) and dialyzed (A_D) samples [31].

Computational studies

Molecular docking

The crystal structure of MAO-primary B was carefully obtained and retrieved from the Protein Data Bank (PDB) (http://www.rcsb.org; ID: 2v5z; resolution: 1.60). This enzyme consists of two chains: A (499 residues) and B (494 residues). The Protein Preparation Wizard tool was used to remove water molecules, alter side-chain protonation states, and add missing hydrogen atoms to the crystal structures for optimization and reduction. The required proteins were digested and processed for grid construction. The centroid of the cocrystal ligand was used as the default parameter to build the grid. The compounds were prepared for docking using the Ligprep tool and an OPLS-2005 force field [32–35].

Molecular dynamics

The Desmond package (Desmond V 7.2) was installed at Dell Inc. A precision 7820 Tower Workstation with Intel Xenon® Silver 4210R and NVIDIA Corporation GP104GL (RTX A 4000) graphics, configured by the Ubuntu 22.04.1 LTS 64-bit, was used to perform MD for the lowest docking pose of compound BCH2. Parameters for the MD investigation including solvent simulation box shape, size, barometer, thermostat parameters, and long- and short-range interaction calculations were described in earlier studies [36]. Root-mean-square deviation (RMSD), root-mean-square fluctuation (RMSF), and protein–ligand contact analyses across all C atoms were built during the 100 ns MD simulation to evaluate the domain correlations. To investigate the protein–ligand interaction dynamics after the MD run, the MD trajectory was selected at 100 ps intervals with 1000 frames generated for each [37].

Results and discussion

MAO-A and MAO-B inhibition studies

At a concentration of 10 µM, seven compounds showed low residual activity for MAO-B, less than 50% for MAO-B, and three compounds showed less than 50% residual activity for MAO-A (Fig. 2, Table 1). BCH2 showed the best inhibitory activity against MAO-B with an IC_{50} value of 0.80 µM, followed by BCH4 (IC_{50} = 1.11 µM); BCH6 was identified as the best inhibitor against MAO-A with an IC_{50} value of 1.63 µM, but it was a nonselective inhibitor with similar inhibitory activity

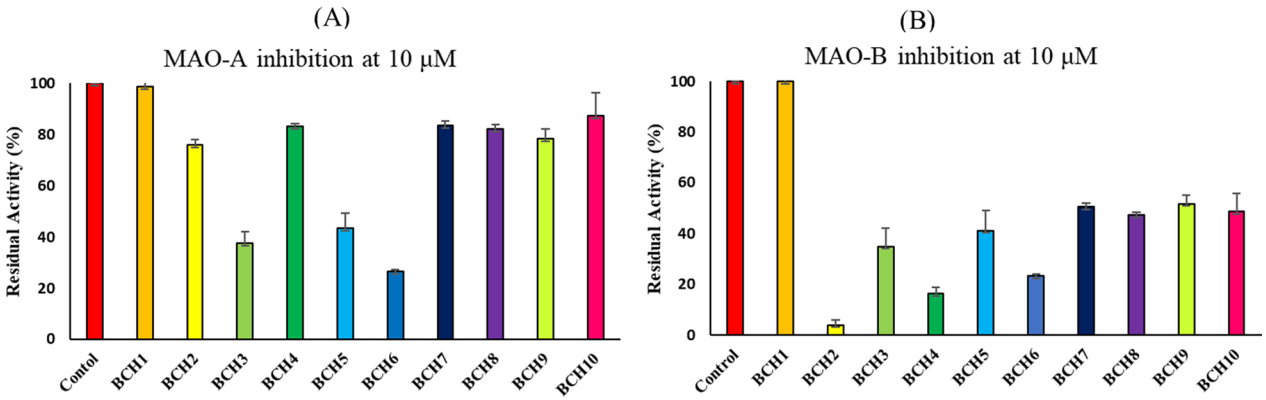

Fig. 2 MAO activity inhibition evaluation of benzimidazole chalcone derivatives

Table 1 Inhibitions of MAO-A and MAO-B by benzimidazole chalcone derivatives[a]

Compound	Residual activity at 10 µM (%)		IC_{50} (µM)		SI
	MAO-A	MAO-B	MAO-A	MAO-B	
BCH1	98.73 ± 10.74	99.95 ± 7.69	> 40	> 40	–
BCH2	76.00 ± 1.89	4.05 ± 1.91	35.29 ± 4.55	0.80 ± 0.0094	44.11
BCH3	37.50 ± 4.65	35.05 ± 7.27	5.59 ± 1.12	4.83 ± 0.76	1.16
BCH4	83.33 ± 0.94	16.48 ± 2.41	27.17 ± 0.14	1.11 ± 0.17	24.48
BCH5	43.38 ± 6.08	41.3 ± 7.69	8.39 ± 0.70	6.87 ± 1.79	1.22
BCH6	26.63 ± 0.77	23.36 ± 0.58	1.63 ± 0.10	2.04 ± 0.13	0.80
BCH7	83.70 ± 1.54	50.54 ± 1.52	> 40	10.94 ± 0.89	3.66
BCH8	82.28 ± 1.79	47.52 ± 0.98	> 40	8.32 ± 1.53	4.81
BCH9	78.48 ± 3.59	51.76 ± 3.33	> 40	10.02 ± 0.30	3.99
BCH10	87.5 ± 8.84	48.78 ± 6.90	> 40	11.09 ± 0.07	3.61
Toloxatone	–	–	1.646 ± 0.094	–	
Lazabemide	–	–	–	0.073 ± 0.0013	
Clorgyline	–	–	0.0079 ± 0.00094	–	
Pargyline	–	–	–	0.11 ± 0.011	

[a] Results are presented as the means ± standard error of duplicate or triplicate experiments

[b] Selectivity index (SI) are calculated for MAO-B using IC_{50} values, i.e., IC_{50} of MAO-A/ IC_{50} of MAO-B

for MAO-B (IC_{50} value = 2.04). Regarding the SI value, BCH2 exhibited the highest value of 44.11, followed by BCH4 (SI = 24.48). BCH2 with *ortho*-Cl on the B ring showed the best MAO-B inhibitory function, followed by BCH4 with *ortho*-Br. BCH2 and BCH4 showed more than 50.0 and 36.0 times, respectively, higher MAO-B inhibitory activity than the parental compound BCH1 (IC_{50} > 40 μM) (Table 1). In comparison with *ortho*-substituents, the inhibitory activities increased in the order, -Cl > -Br > -F > -H. In addition, the *ortho*-site of the B ring showed better inhibitory activity than *para*-site (BCH2 > BCH3; BCH4 > BCH5). Uniquely, BCH6 with *ortho*-F of the B ring inhibited both MAO-A and MAO-B (IC_{50} = 2.04 μM) to a similar degree. Overall, the halogen substituents exhibited better inhibitory capabilities than the alkyl groups, methoxy groups, and piperidine.

Enzyme kinetics

Enzyme and inhibition kinetics were analyzed at five substrate concentrations and three inhibitor concentrations. According to the Lineweaver–Burk plots, BCH2 appeared to be a competitive MAO-B inhibitor (Fig. 3A). In addition, secondary plots showed that the K_i value was 0.25 ± 0.014 μM. (Fig. 3B). These results suggested that BCH2 acts as a competitive MAO-B inhibitor.

Reversibility studies

The reversibility of BCH2 MAO-B inhibition was analyzed using the dialysis method. In these experiments, the compound BCH2 concentration used was two times the IC_{50} (1.6 μM). The recovery pattern was compared by using undialyzed (A_U) and dialyzed (A_D) relative activities after 30 min of pre-incubation. The compound BCH2 recovered from 24.14% to 57.10% (Fig. 4). The recovery of

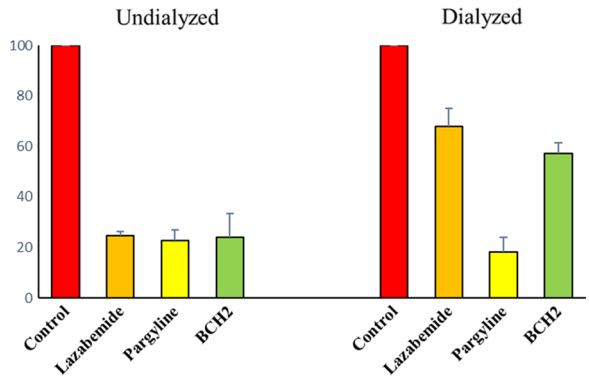

Fig. 4 Recovery of MAO-B inhibition by BCH2 using dialysis experiments

the compound was similar to that of lazabemide (reversible type, from 22.66% to 67.94%) and could be distinguished from that of pargyline (irreversible type, from 22.22% to 18.25%). These results indicated that BCH2 is a reversible MAO-B inhibitor.

Molecular docking

Using the Glide module, we docked the hit molecule into the binding cavity of protein 2V5Z. The lead molecule BCH2 showed a docking score (XP mode) of around -10.152 kcal/mol, which was comparable to that of safinamide's score (− 11.684 kcal/mol), whereas the least active BCH1 showed − 9.198 kcal/mol. The hit was obtained through pi-pi stacking with Phe343 (Fig. 5A). Other interactions included hydrophobic interactions with Phe103, Pro102, Tyr60, Tyr435, Tyr398, Leu164, Tyr326, Leu328, Cys172, Ile198, and Ile199. A 2D interaction diagram of the hit molecules is shown in Fig. 5A. We found that the chloro phenyl ring in BCH2 was close to

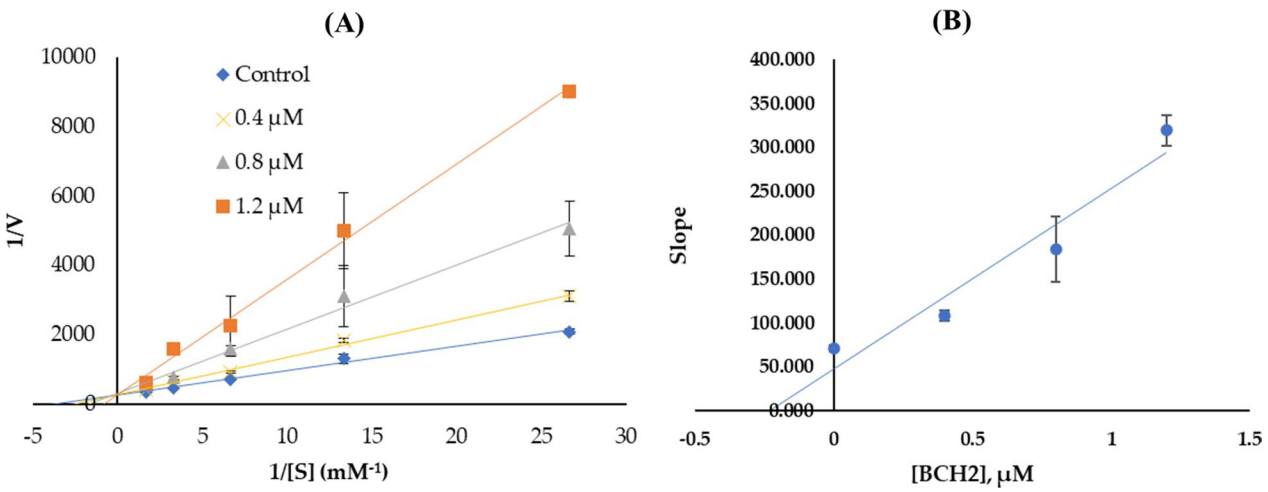

Fig. 3 Lineweaver–Burk plots for MAO-B inhibition by BCH2 **A**, and the respective secondary plot **B** of the slopes vs. inhibitor concentrations

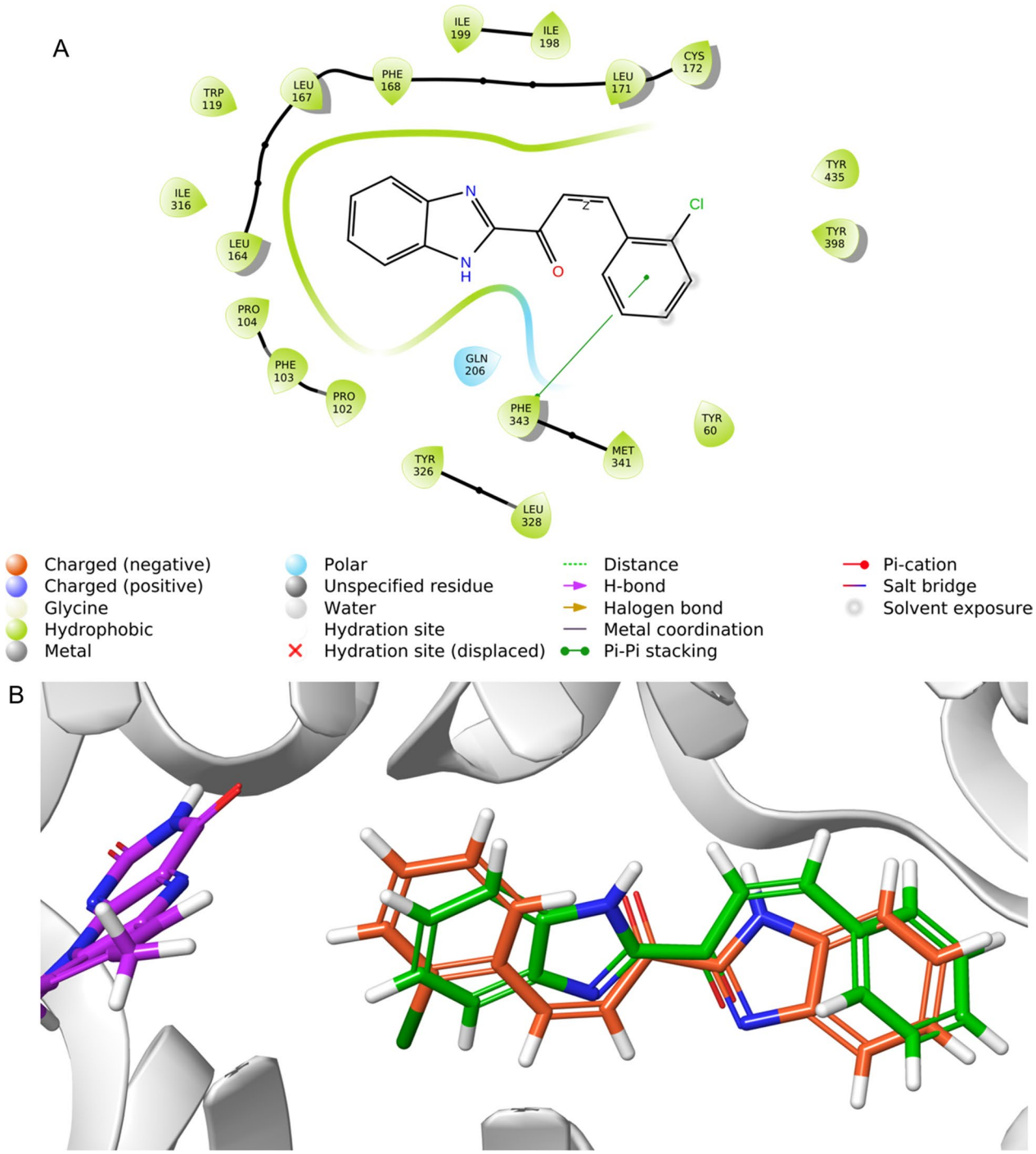

Fig. 5. 2D **A** and 3D **B** ligand interactions with the lead compound BCH2. BCH2 and FAD were shown as red–orange and purple, respectively. For comparison, BCH1 was provided as green

FAD while the benzimidazole moiety in BCH1 was close to FAD, when comparing the docking contacts of the two compounds (Fig. 5B). The result showed that halogen alterations changed the orientation of BCH2, enhancing interaction.

Molecular dynamics

In drug discovery research, the MD simulation is used to simulate the dynamic behaviors of a protein–ligand complex as closely or as realistically as possible. This allows researchers to quickly obtain energy information

on how proteins and ligands interact. In this study, BCH2 was modeled at the binding site of MAO-B protein using MD modeling by simulating according to the biological situations. RMSD, RMSF, and protein–ligand interactions were calculated using MD trajectories. Numerous MD trajectory data analyses of the BCH2-MAO-B complex are shown in Fig. 6. Both complexes were simulated using water molecules. With RMSD values for protein C_α atoms in complex with ligand ranging from 1.2 to 3.6 Å, the RMSD plot (Fig. 6A) showed a stable ligand–protein complex during the simulation duration, while BCH1's ligand RMSD ranged from 1.3 to 5.9 Å. The greatest RMSD for BCH2 and BCH1 (Fig. 7) was 3.6 Å and 5.9 Å at 35 ns and 80–90 ns, respectively. During the simulation, it appeared that the BCH1 phenyl ring deviated more from the norm than the halogen-substituted phenyl ring. For compound BCH2, RMSD relative to the protein, the ligand RMSD ranged from 2.0 to 3.6. Apart from a small change, the RMSD of the simulation study for BCH2 was found to be constant. The maximum protein RMSD was measured at 20 ns, where the RMSD value was found to be 3.6 Å; after 45 ns, the protein begins to stabilize. The RMSD plot demonstrates that the ligand is stable with respect to the protein and its binding site. The

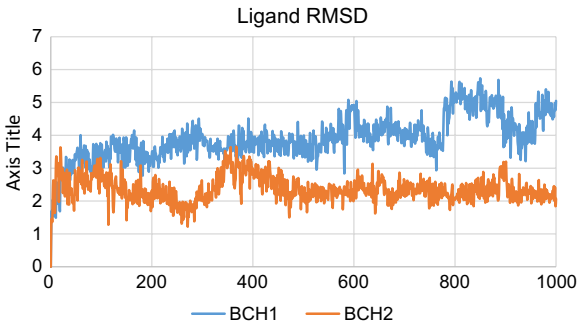

Fig. 7 Comparison ligand RMSD of **BCH1** (blue) and **BCH2** (orange)

simulation also evaluated the adaptability of the protein system by computing the RMSF for each amino acid residue of the protein. The RMSF plot (Fig. 6B) indicates very fewer fluctuations (0.6–2.0 Å) and higher fluctuations in the N- and C-terminal residues. Tyr60 (0.544 Å), Glu84 (1.128 Å), Pro102 (2.042 Å), Pro104 (1.507 Å), Leu164 (0.727 Å), Leu167 (0.658 Å), Phe168 (0.658 Å), Leu171 (0.7 Å), Ile198 (0.89 Å), Ile199 (1.201 Å), Ser200 (0.99 Å), Thr201 (0.938 Å), Gln206 (0.719 Å), Ile316 (0.88 Å), Tyr326 (0.768 Å), Leu328 (0.822 Å), Phe343 (0.69 Å),

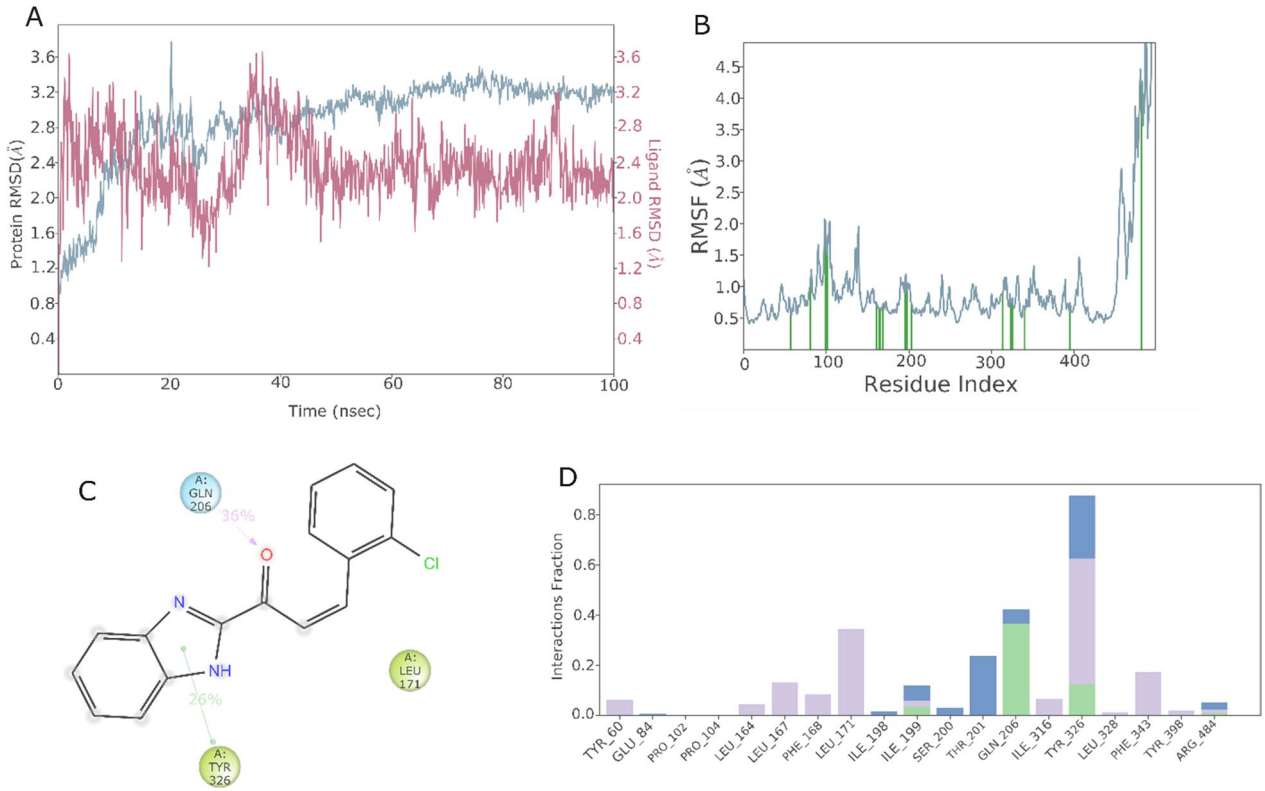

Fig. 6 MD simulation analysis of the BCH2-MAO-B complex. **A** RMSD of protein (blue) and BCH2 (red); **B** RMSF for amino acid residues of the protein; **C** Diagram of 2-D Interaction; **D** Plot of Protein–ligand interactions

Table 2 Computational studies of benzimidazole chalcone derivatives

CODE	Log S (Log mol/L)	GI Absorption	BBB perm	Metabolism
BCH1	− 4.03	High	yes	CYP1A2, CYP2C19, CYP2C9 inhibitor
BCH2	− 4.61	High	yes	CYP1A2, CYP2C19, CYP2C9 inhibitor
BCH3	− 4.61	High	yes	CYP1A2, CYP2C19, CYP2C9 inhibitor
BCH4	− 4.92	High	yes	CYP1A2, CYP2C19, CYP2C9 inhibitor
BCH5	− 4.92	High	yes	CYP1A2, CYP2C19, CYP2C9 inhibitor
BCH6	− 4.17	High	yes	CYP1A2, CYP2C19 inhibitor
BCH7	− 4.17	High	yes	CYP1A2, CYP2C19, CYP2C9 inhibitor
BCH8	− 4.58	High	yes	CYP1A2, CYP2C19, CYP2C9, CYP2D6 inhibitor
BCH9	− 4.31	High	yes	CYP1A2, CYP2C19, CYP2C9 inhibitor
BCH10	− 4.07	High	yes	CYP1A2, CYP2C19, CYP2C9, CYP2D6 inhibitor

The pharmacokinetic properties were calculated in silico using the online database [a]SwissADME (http://www.swissadme.ch/)

and Tyr398 (0.745 Å) were the 18 amino acid residues with which the ligand interacted. Hydrophobicity, water bridges, and hydrogen bonding are the three main classifications in protein–ligand contact. These interactions in the ligand–protein complexes are shown in Fig. 6C and D. Gln206 is involved in a hydrogen bonding with the carbonyl group of BCH2 with a participation strength of 36%, while Tyr326 participates with 26% strength in a pi-pi stack interaction in 2D. MD simulations help understanding the binding patterns, because the physiological environment is more accurately mirrored. Trajectory analysis and overall MD simulations indicated that the lead molecule inhibited MAO-B.

ADME prediction

Solubility is an important feature determining absorbance for drug discovery schemes that intend to develop drugs for oral delivery. In addition, a medication intended for parenteral administration must be sufficiently dissolved in water to provide an adequate amount of the bioactive component in a modest pharmacological dosage.

Understanding the mechanisms by which chemicals interact with cytochrome P450 (CYP) is crucial. This superfamily of isoenzymes plays an important role in drug disposal through metabolic biotransformation. On average, the five main isoforms represent the substrates for 50–90% of the therapeutic compounds (CYP1A2, CYP2C19, CYP2C9, CYP2D6, and CYP3A4). As these isoenzymes are inhibited, there is poor clearance and retention of the drug or its metabolites, which can result in toxic or undesirable side effects. This is one of the main causes of drug-drug interactions linked to pharmacokinetics. Nonetheless, interactions between all compounds and cytochrome isoenzymes were apparent (Table 2). Blood–brain barrier (BBB) permeability is essential for the treatment of neurodegenerative diseases. All the subsequent medications showed comparable BB permeation. The bulk of these compounds exhibits favorable ADME properties, making them viable candidates [38].

Collectively, we assessed the inhibitory potential of the 10 synthesized benzimidazole chalcone derivatives (**BCH1-BCH10**) against MAO-A and MAO-B. Most compounds exhibited selective MAO-B inhibitory actions. With an IC_{50} value of 0.80 µM and an SI value of 44.11, **BCH2** presented the highest selective MAO-B inhibition, followed by **BCH4** (IC_{50} = 1.11, SI = 24.48). According to the kinetic and reversibility tests, **BCH2** is a competitive and reversible inhibitor of MAO-B. An MD study also predicted that the addition of halogens to the benzimidazole chalcone framework might strengthen MAO-B inhibition. As a result, our study suggests that **BCH2** is a potential candidate for the treatment of neurodegenerative diseases such as AD.

Acknowledgements

Not applicable.

Author contributions

Conceptualization: HK, BM; Synthesis: AK, SK, STS, LKP; Biological assay: JL; Docking analysis: PU; Writing-original draft preparation: AK, JL; Writing-review and editing: BM, HK; Supervision: HK. All authors have read and approved the final manuscript.

Funding

This work was supported by a Research Promotion Program of SCNU.

Availability of data and materials

All data generated or analyzed during the present study are included in this published article.

Declarations

Competing interests

The authors declare that they have no competing interests.

Received: 14 April 2023 Accepted: 29 May 2023
Published online: 17 June 2023

References

1. Kumar A, Sudevan ST, Nair AS, Singh AK, Kumar S, Jose J, Behl T, Mangalathillam S, Mathew B, Kim H (2023) Current and future nano-carrier-based approaches in the treatment of Alzheimer's disease. Brain Sci 13(2):213
2. Bhawna KA, Bhatia M, Kapoor A, Kumar P, Kumar S (2022) Monoamine oxidase inhibitors: a concise review with special emphasis on structure-activity relationship studies. Eur J Med Chem 242:114655
3. Guglielmi P, Carradori S, D'Agostino I, Campestre C, Petzer JP (2022) An updated patent review on monoamine oxidase (MAO) inhibitors. Expert Opin Ther Pat 32(8):849–883
4. Rinaldi D, Alborghetti M, Bianchini E, Sforza M, Galli S, Pontieri FE (2022) Monoamine-oxidase type B-Inhibitors and cognitive functions in Parkinson's disease: beyond the Primary Mechanism of Action. Curr Neuropharmacol. https://doi.org/10.2174/1570159X20666220905102144
5. Chaurasiya ND, Leon F, Muhammad I, Tekwani BL (2022) Natural products inhibitors of monoamine oxidases-potential new drug leads for neuroprotection, neurological disorders, and neuroblastoma. Molecules 27(13):4297
6. Tripathi RKP, Ayyannan SR (2019) Monoamine oxidase-B inhibitors as potential neurotherapeutic agents: an overview and update. Med Res Rev 39(5):1603–1706
7. Manzoor S, Hoda N (2020) A comprehensive review of monoamine oxidase inhibitors as anti-Alzheimer's disease agents: a review. Eur J Med Chem 206:112787
8. Mathew B, Parambi DGT, Mathew GE, Uddin MS, Inasu ST, Kim H, Marathakam A, Unnikrishnan MK, Carradori S (2019) Emerging therapeutic potentials of dual-acting MAO and AChE inhibitors in Alzheimer's and Parkinson's diseases. Arch Pharm (Weinheim) 352(11):e1900177
9. Faheem M, Rathaur A, Pandey A, Singh VK, Tiwari AK (2020) A review on the modern synthetic approach of benzimidazole candidate. ChemistrySelect 5(13):3981–3994. https://doi.org/10.1002/slct.201904832
10. Feng LS, Su WQ, Cheng JB, Xiao T, Li HZ, Chen DA, Zhang ZL (2022) Benzimidazole hybrids as anticancer drugs: an updated review on anticancer properties, structure-activity relationship, and mechanisms of action (2019–2021). Arch Pharm (Weinheim). 355(6):e2200051
11. Ali AM, Tawfik SS, Mostafa AS, Massoud MAM (2022) Benzimidazole-based protein kinase inhibitors: current perspectives in targeted cancer therapy. Chem Biol Drug Des 100(5):656–673
12. Tahlan S, Kumar S, Narasimhan B (2019) Pharmacological significance of heterocyclic 1H-Benzimidazole scaffolds: a review. BMC Chem 13(1):1–21. https://doi.org/10.1186/s13065-019-0625-4
13. Kumar S, Oh JM, Abdelgawad MA, Abourehab MAS, Tengli AK, Singh AK, Ahmad I, Patel H, Mathew B, Kim H (2023) Development of isopropyl-tailed chalcones as a new class of selective MAO-B Inhibitors for the treatment of Parkinson's disorder. ACS Omega 8(7):6908–6917
14. Sudevan ST, Oh JM, Abdelgawad MA, Abourehab MAS, Rangarajan TM, Kumar S, Ahmad I, Patel H, Kim H, Mathew B (2022) Introduction of benzyloxy pharmacophore into aryl/heteroaryl chalcone motifs as a new class of monoamine oxidase B inhibitors. Sci Rep 12(1):22404
15. Sang Z, Song Q, Cao Z, Deng Y, Zhang L (2022) Design, synthesis, and evaluation of chalcone-vitamin E-donepezil hybrids as multi-target-directed ligands for the treatment of Alzheimer's disease. J Enzyme Inhib Med Chem 37(1):69–85
16. Rehuman NA, Oh JM, Abdelgawad MA, Beshr EAM, Abourehab MAS, Gambacorta N, Nicolotti O, Jat RK, Kim H, Mathew B (2022) Development of halogenated-chalcones bearing with dimethoxy phenyl head as monoamine oxidase-B Inhibitors. Pharmaceuticals (Basel) 15(9):1152
17. Mathew B, Oh JM, Khames A, Abdelgawad MA, Rangarajan TM, Nath LR, Agoni C, Soliman MES, Mathew GE, Kim H (2021) Replacement of chalcone-ethers with chalcone-thioethers as potent and highly selective monoamine oxidase-B Inhibitors and their protein-ligand Interactions. Pharmaceuticals (Basel) 14(11):1148. https://doi.org/10.3390/ph14111148
18. Zaib S, Rizvi SU, Aslam S, Ahmad M, Ali Abid SM, Al-Rashida M, Iqbal J (2015) Quinolinyl-thienyl chalcones as monoamine oxidase inhibitors and their *in silico* modeling studies. Med Chem 11(6):580–589. https://doi.org/10.2174/1573406410666141226131252
19. Jasim HA, Nahar L, Jasim MA, Moore SA, Ritchie KJ, Sarker SD (2021) Chalcones: synthetic chemistry follows where nature leads. Biomolecules 11(8):1203
20. Elkanzi NAA, Hrichi H, Alolayan RA, Derafa W, Zahou FM, Bakr RB (2022) Synthesis of chalcones derivatives and their biological activities: a review. ACS Omega 7(32):27769–27786
21. Mathew B, Suresh J, Vinod D (2013) Antitumour activity of 5-[(2*E*)-1-(1*H*-benzimidazol-2-yl)-3-substituted phenylprop-2-en-1-ylidene] pyrimidine-2,4,6(1*H*,3*H*,5*H*)-triones against Dalton's ascitic lymphoma in mice. Med Chem Res 22:3911–3917
22. Mathew B, Suresh J, Anbazhagan S (2016) Development of novel (1-H) benzimidazole bearing pyrimidine-trione based MAO-A inhibitors: synthesis, docking studies and antidepressant activity. J Saudi Chem Soc 20:S132–S139
23. Mathew B, Suresh J, Anbazhagan S, Chidambaranathan N (2016) Discovery of some novel imines of 2-amino, 5-thio, 1, 3, 4-thiadiazole as mucomembranous protector: synthesis, anti-oxidant activity and in silico PASS approach. J Saudi Chem Soc 20:S426–S432
24. Oh JM, Rangarajan TM, Chaudhary R, Singh RP, Singh M, Singh RP, Tondo AR, Gambacorta N, Nicolotti O, Mathew B, Kim H (2020) Novel class of chalcone oxime ethers as potent monoamine oxidase-B and acetylcholinesterase inhibitors. Molecules 25(10):2356
25. Lee HW, Ryu HW, Kang MG, Park D, Lee H, Shin HM, Oh SR, Kim H (2017) Potent inhibition of monoamine oxidase A by decursin from *Angelica gigas* Nakai and by wogonin from *Scutellaria baicalensis* Georgi. Int J Biol Macromol 97:598–605
26. Oh JM, Kang Y, Hwang JH, Park JH, Shin WH, Mun SK, Lee JU, Yee ST, Kim H (2022) Synthesis of 4-substituted benzyl-2-triazole-linked-tryptamine-paeonol derivatives and evaluation of their selective inhibitions against butyrylcholinesterase and monoamine oxidase-B. Int J Biol Macromol 217:910–921
27. Baek SC, Park MH, Ryu HW, Lee JP, Kang MG, Park D, Park CM, Oh SR, Kim H (2019) Rhamnocitrin isolated from *Prunus padus* var. seoulensis: a potent and selective reversible inhibitor of human monoamine oxidase A. Bioorg Chem 83:317–325
28. Baek SC, Lee HW, Ryu HW, Kang MG, Park D, Kim SH, Cho ML, Oh SR, Kim H (2018) Selective inhibition of monoamine oxidase A by hispidol. Bioorg Med Chem Lett 28(4):584–588
29. Oh JM, Jang HJ, Kim WJ, Kang MG, Baek SC, Lee JP, Park D, Oh SR, Kim H (2020) Calycosin and 8-*O*-methylretusin isolated from *Maackia amurensis* as potent and selective reversible inhibitors of human monoamine oxidase-B. Int J Biol Macromol 151:441–448
30. Rehuman NA, Oh JM, Nath LR, Khames A, Abdelgawad MA, Gambacorta N, Nicolotti O, Jat RK, Kim H, Mathew B (2021) Halogenated coumarin-chalcones as multifunctional monoamine oxidase-B and butyrylcholinesterase inhibitors. ACS Omega 6(42):28182–28193
31. Vishal PK, Oh JM, Khames A, Abdelgawad MA, Nair AS, Nath LR, Gambacorta N, Ciriaco F, Nicolotti O, Kim H, Mathew B (2021) Trimethoxylated halogenated chalcones as dual inhibitors of MAO-B and BACE-1 for the treatment of neurodegenerative disorders. Pharmaceutics 13(6):850
32. Schrödinger Release 2021–4: LigPrep, Schrödinger, LLC, New York, NY, 2021.
33. Schrödinger Release 2021–4: Glide, Schrödinger, LLC, New York, NY, 2021.
34. Schrödinger Release 2021–4: Protein Preparation Wizard; Epik, Schrödinger, LLC, New York, NY, 2021; Impact, Schrödinger, LLC, New York, NY, 2021; Prime, Schrödinger, LLC, New York, NY, 2021.
35. Friesner RA, Banks JL, Murphy RB, Halgren TA, Klicic JJ, Mainz DT, Repasky MP, Knoll EH, Shelley M, Perry JK, Shaw DE, Francis P, Shenkin PS (2004) Glide: a new approach for rapid, accurate docking and scoring 1. Method and assessment of docking accuracy. J Med Chem 47(7):1739–1749. https://doi.org/10.1021/jm0306430
36. Kumar S, Manoharan A, Jayalakshmi J, Abdelgawad MA, Mahdi WA, Alshehri S, Ghoneim MM, Pappachen LK, Zachariah SM, Aneesh TP, Mathew B (2023) Exploiting butyrylcholinesterase inhibitors through a combined 3-D pharmacophore modeling, QSAR, molecular docking, and molecular dynamics investigation. RSC Adv. 13(14):9513–9529
37. Desmond Molecular Dynamics System, D. E. Shaw Research, New York, NY, 2021 Maestro-Desmond interoperability tools. Schrödinger, New York, NY, 2021.

38. Daina A, Michielin O, Zoete V (2017) SwissADME: a free web tool to evaluate pharmacokinetics, drug-likeness and medicinal chemistry friendliness of small molecules. Sci Rep 7:42717

Publisher's Note